Journal of Alloys and Compounds 509 (2011) 4138–4145

Contents lists available at ScienceDirect

Journal of Alloys and Compounds

journal homepage: www.elsevier.com/locate/jallcom

Effect of solution treatment on the strength and fracture toughness of aluminum alloy 7050

N.M. Han, X.M. Zhang*, S.D. Liu, D.G. He, R. Zhang

School of Materials Science and Engineering, Central South University, Changsha, Hunan Province 410083, PR China

ARTICLE INFO

Article history:
Received 26 November 2010
Received in revised form 4 January 2011
Accepted 4 January 2011
Available online 5 January 2011

Keywords:
Aluminum alloy 7050
Solution treatment
Tensile property
Fracture toughness

ABSTRACT

The effect of the solution treatment on the tensile property and fracture toughness of aluminum alloy 7050 were investigated by means of optical microscopy (OM), scanning electron microscopy (SEM), transmission electron microscopy (TEM), tensile test and the plane-strain fracture toughness test. The results show that with increasing single-stage solution temperature, the volume fraction of the residual phase decreases, but the volume fraction of the recrystallized grains and the size of the sub-grains increase. Thus, the strength and fracture toughness of the single-stage solution treated samples increase first and then decrease. The enhanced solution treated samples result in an improved dissolution of the residual phase, a lower recrystallized grains fraction and smaller sub-grains, which leads to a higher strength and fracture toughness than that of the single-stage solution treated samples. The grain structure of the high temperature pre-precipitation treated samples is similar to that of the enhanced solution treated samples. However, the high temperature pre-precipitation treated samples exhibit a lower strength and fracture toughness, due to a mass of AlZnMgCu phase precipitating from the matrix.

1. Introduction

The 7xxx series aluminum alloy thick plates have been widely used for manufacturing of aircraft structural wing components free from welding and riveting [1,2]. Compared to the conventional aluminum alloys such as 2xxx and Al–Li alloys, the 7xxx series aluminum alloy exhibits a good combination between the strength and fracture toughness [3]. Thus, many investigations have been carried out on the microstructures and properties of the 7xxx series aluminum alloy [4,5].

In order to obtain improved mechanical properties, aluminum alloys are often subjected to different heat treatments. Generally, the solution treatment is a primary and key step [6–8]. During the solution treatment, the soluble phase formed during solidification can be re-dissolved into the matrix. At a higher solution temperature, the soluble phase can re-dissolve more sufficiently. However, for the single-stage solution treatment, the solution temperature must be below the incipient melting point for each specific composition. Otherwise, the alloy may be overburnt. The specimen treated with an enhanced solution exhibit a significant increase in the yield strength and fracture toughness because the residual phase can be re-dissolved into the matrix beyond the overburning temperature of the single-stage solution treatment [9,10]. The high temperature pre-precipitation treatment increases the resistance to intergranular corrosion and exfoliation corrosion, but decreases the mechanical properties [11]. However, the effect of the high temperature pre-precipitation treatment (HTPT) on the fracture toughness has been seldom reported. In a word, the study of the effect of the solution treatment is necessary and is contributed to get an improved comprehensive property of the 7xxx series aluminum alloy.

In this paper, the effects of the single-stage solution treatment (SST), the enhanced solution treatment (EST) and the high temperature pre-precipitation treatment (HTPT) on the tensile properties and fracture toughness of the 7050 aluminum alloy were studied. These results can give indispensable information for optimizing the solution processing parameters.

2. Experimental procedure

The present study was carried out on the 80 mm thick hot rolled 7050 aluminum alloy plate with chemical composition of Al–6.06% Zn–2.20% Mg–2.12% Cu–0.11% Zr–0.08% Fe–0.04% Si (wt.%). The plates were solution treated in air furnace, quenched in room temperature water, and then aged at 121 °C for 6 h and 163 °C for 12 h. The solution treatment procedures were listed in details in Table 1.

The samples for metallographic observation were prepared through a conventional mechanical polishing and followed by etching with Graff Seagent solution (1 mL HF, 16 mL HNO_3, 3 g CrO_3 and 83 mL water), which give a good decoration of the recrystallized grains [12]. The morphology of the residual phase was examined on Sirion 200 scanning electron microscopy (SEM). The second phase particles were identified by energy dispersive X-ray spectrometry (EDX). The volume fraction of the recrystallized grains and the second phase particles were measured on the optical micrographs and the SEM micrographs by using point counting with a grid

* Corresponding author. Tel.: +86 731 88830 265; fax: +86 731 88830 265.
E-mail address: xmzhang_cn@yahoo.cn (X.M. Zhang).

0925-8388/$ – see front matter © 2011 Elsevier B.V. All rights reserved.
doi:10.1016/j.jallcom.2011.01.005

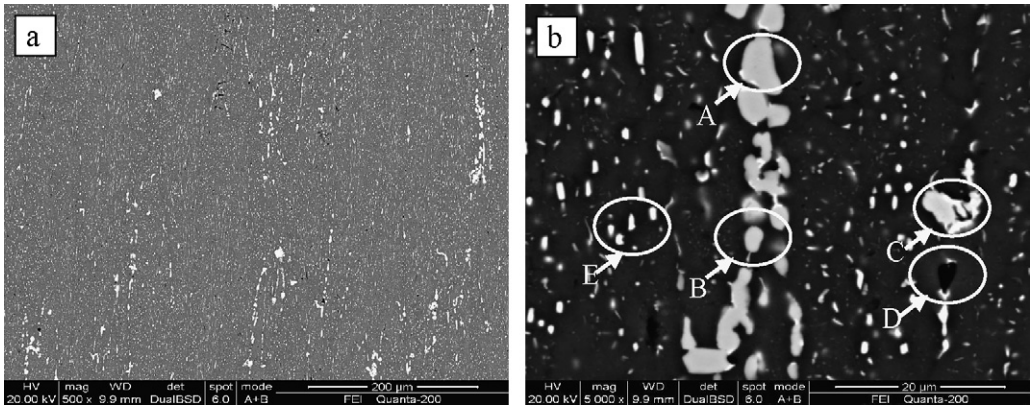

Fig. 1. Morphologies of the second phase particles of the 7050 aluminum alloy rolled plate (a) 500×; and (b) 5000×.

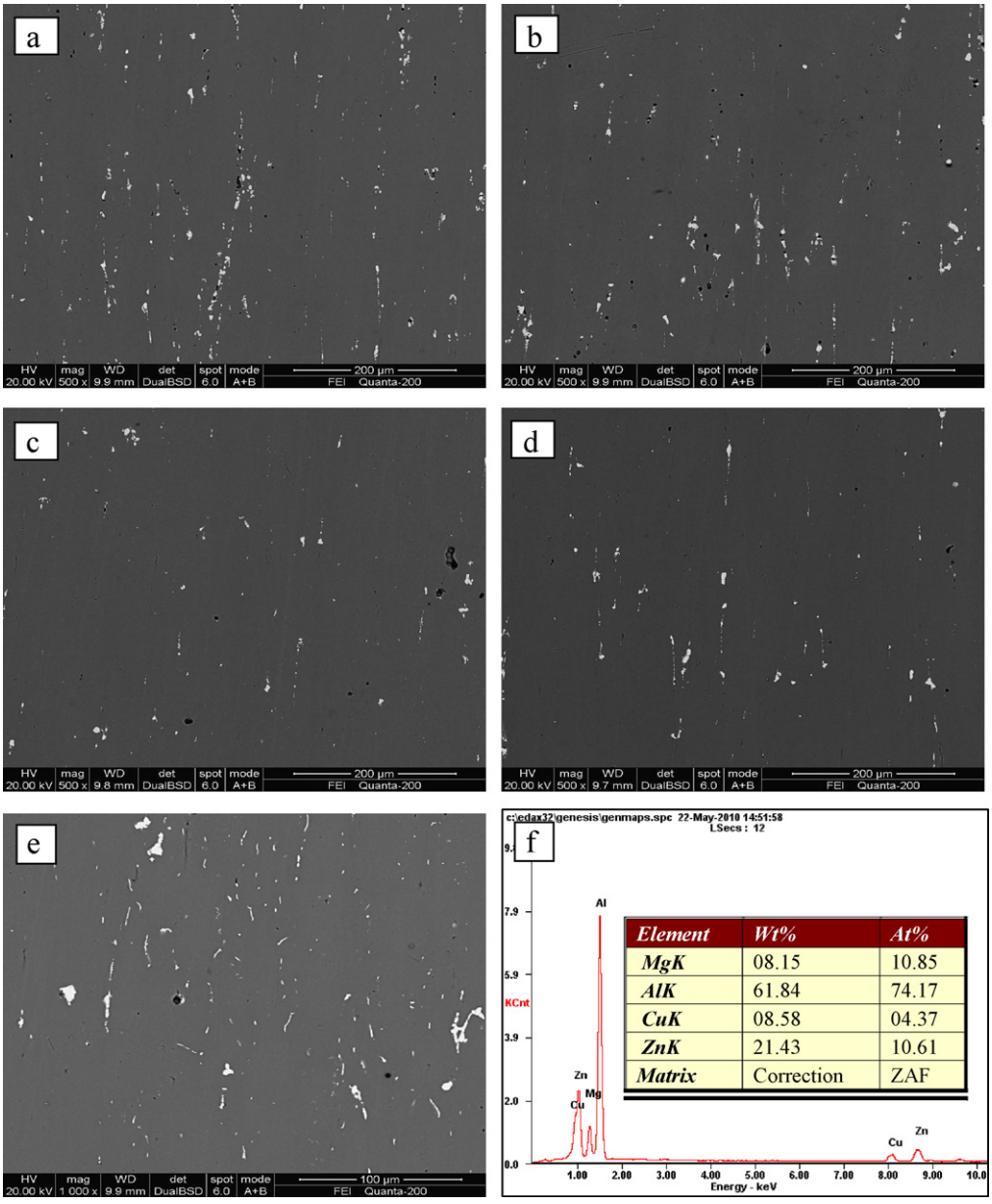

Fig. 2. Typical micrographs of the 7050 aluminum alloy solution treated at different conditions (a) SST450; (b) SST470; (c) SST490; (d) EST; (e) HTPT; and (f) EDX of the fine phase in the HTPT sample.

Table 1
Solution treatment schedules of the 7050 aluminum alloy rolled plate.

Test number	First step	Ramp rate	Second step	Ramp rate	Third step
SST440	440 °C/2.5 h				
SST450	450 °C/2.5 h				
SST460	460 °C/2.5 h				
SST470	470 °C/2.5 h				
SST480	480 °C/2.5 h				
SST490	490 °C/2.5 h				
EST	450 °C/1.5 h	60 °C/h	480 °C/0.5 h		
HTPT	450 °C/1.5 h	60 °C/h	480 °C/0.5 h	30 °C/h	420 °C/0.5 h

Table 2
EDX results of the second phase particles of the 7050 aluminum alloy rolled plate (wt.%).

Point	Al	Zn	Mg	Cu	Fe	Si
A	72.37	6.87	8.78	11.98		
B	60.59		20.14	19.27		
C	74.16			17.33	8.5	
D	15.99		41.60			42.41
E	74.17	10.61	10.85	4.37		

containing 900 points [13]. Six random views of each of specimens were examined. TEM specimens were prepared by the standard twin-jet electropolishing method using 75% methanol and 25% nitric acid solution below −30 °C, and then characterized by Tecnai G220 electron microscopy operated at 200 kV. The plane-strain fracture toughness tests were performed according to the ASTM E399 standard on the compact-tension specimens taken in the L–T orientation. The fracture surfaces of the compact-tension specimens were examined on the SEM. The ambient temperature tensile property tests were performed on CSS-44100 electronic universal testing machine at a tensile velocity of 2 mm/min.

3. Results and discussion

Fig. 1 shows the microstructure of the 7050 aluminum alloy rolled plate. It can be observed that a number of coarse second phase particles distribute along the rolling direction. Except for the spherical particles, other particles appear as irregular-shaped blocks. The EDX analysis reveals that these second particles are AlZnMgCu phase, AlCuMg phase, Fe-rich phase and Si-rich phase (Table 2). Large amounts of fine white phase are distributed homogenously in the matrix (Fig. 1b). According to the EDX analysis, they are also AlZnMgCu phase. Most second phase particles are expected to be dissolved into the matrix by the solution treatment [14]. However, the higher temperature of the solution treatment inevitably increases the percentage of the recrystallized

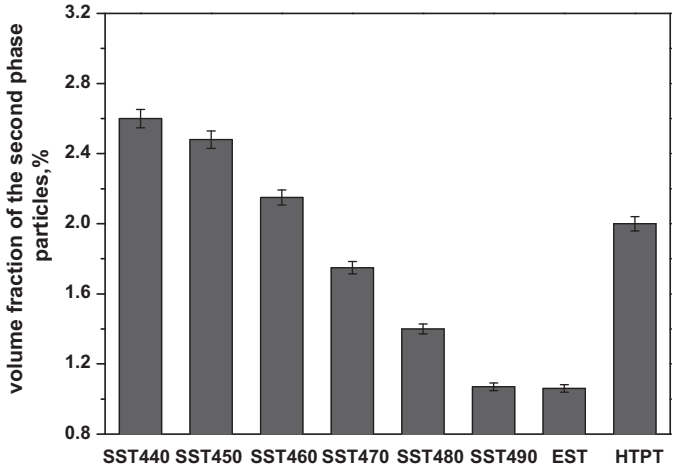

Fig. 3. Volume fraction of the second phase particles of the 7050 aluminum alloy solution treated at different conditions.

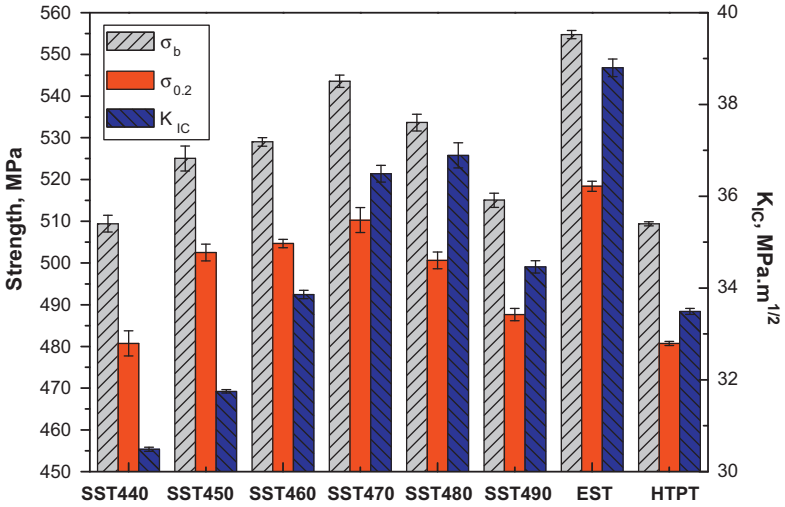

Fig. 4. Tensile properties and fracture toughness of the aged 7050 aluminum alloy solution treated at different conditions.

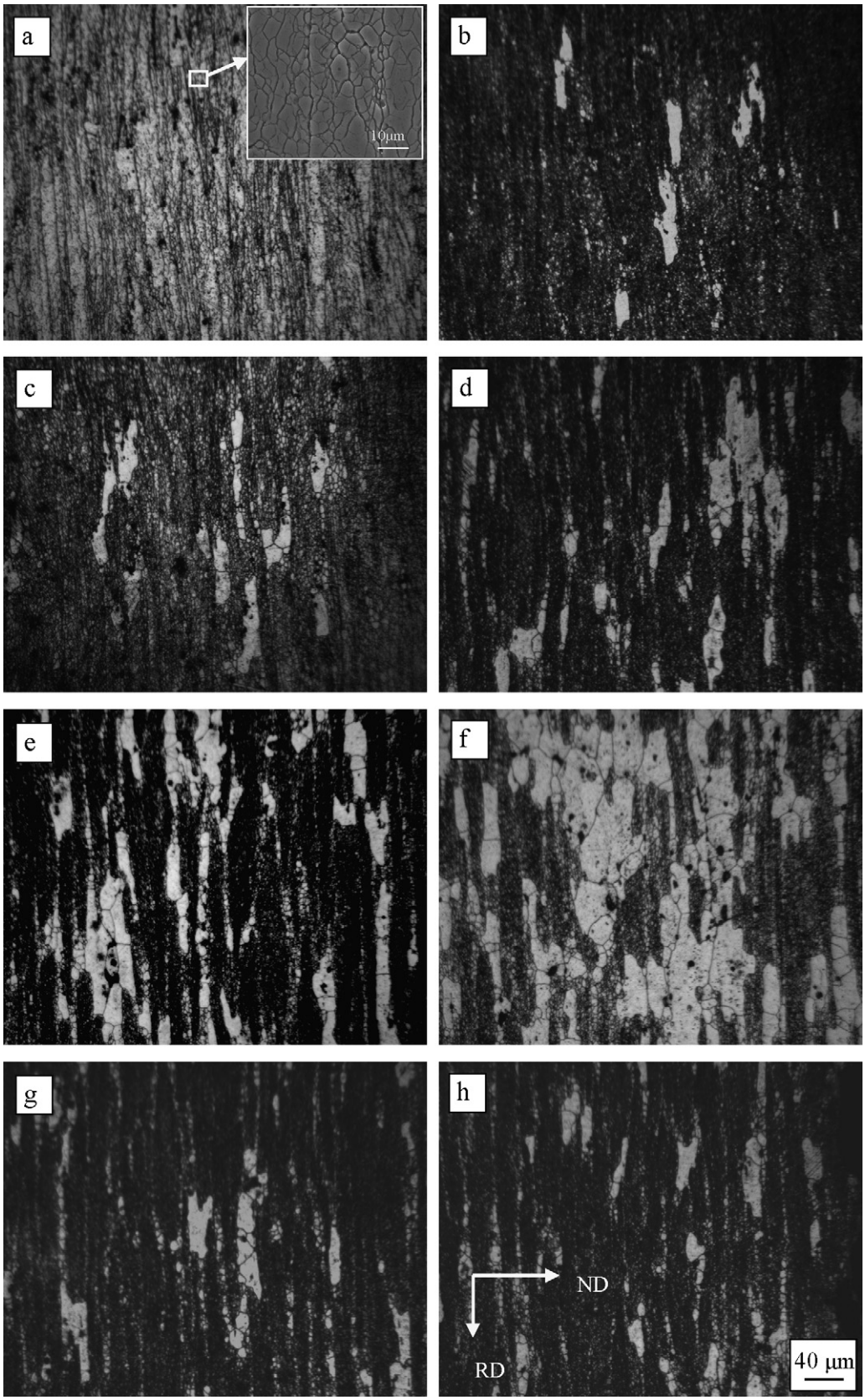

Fig. 5. Optical micrographs of the aged 7050 aluminum alloy solution treated at different conditions (a) SST440; (b) SST450; (c) SST460; (d) SST470; (e) SST480; (f) SST490; (g) EST and (h) HTPT.

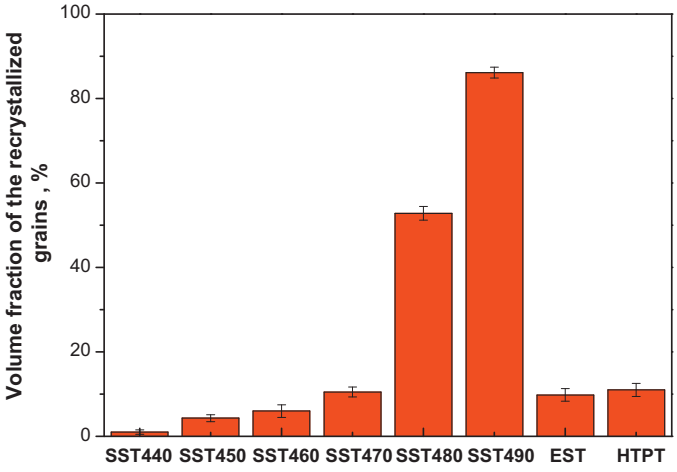

Fig. 6. Volume fraction of the recrystallized grains of the 7050 aluminum alloy solution treated at different conditions.

grains. Therefore, it is necessary to optimize the solution treatment.

The typical micrographs of the 7050 aluminum alloy solution treated at different conditions are shown in Fig. 2. Compared to the 7050 aluminum alloy rolled plate, the fine secondary phase particles are dissolved into the matrix of the SST and EST samples. Fig. 3 presents the volume fraction of the second phase particles of the 7050 aluminum alloy solution treated at different conditions, which decrease with increasing the solution temperature for the SST sample. The comparison of Fig. 2c and d indicates that the EST samples result in the few residual phase particles in the matrix, very similar to those of the 490 °C single-stage solution treated samples (SST490). However, a mass of fine second phases (AlZnMgCu) are observed in the matrix of the HTPT sample. The volume fraction of the second phase particles of the HTPT sample is similar to that of the SST460 sample.

Fig. 4 shows the tensile properties and fracture toughness of the aged 7050 aluminum alloy solution treated at different conditions. For the single-stage solution treated samples, the strength and fracture toughness first increase and then decrease with increasing solution temperature. The ultimate tensile strength (σ_b) and yield strength ($\sigma_{0.2}$) reach their peaks at the solution treatment of 470 °C, and they are 543 MPa and 510 MPa, respectively. While the maximum fracture toughness (K_{IC}) of 36.8 MPa $m^{1/2}$ is obtained at the solution treatment of 480 °C. The σ_b, $\sigma_{0.2}$ and K_{IC} for the EST sample are 554 MPa, 518 MPa and 38.8 MPa $m^{1/2}$ respectively, which are larger than the maximum of the single-stage solution treated samples. However, for the HTPT sample, the properties decline significantly. The σ_b, $\sigma_{0.2}$ and K_{IC} are 509 MPa, 480 MPa and 33.4 MPa $m^{1/2}$, respectively.

Fig. 5 presents the optical micrographs of the aged 7050 aluminum alloy solution treated at different conditions. Fibrous structures consisting of sub-grains are observed in the SST440 sample (Fig. 5a); while partial recrystallized microstructures are observed in the SST450 sample (Fig. 5b). Large elongated bright areas are the recrystallized regions which are aligned parallel to the rolling direction, and the black areas consist of sub-grains. The volume fraction of the recrystallized grains of the 7050 aluminum alloy with different solution treatments is shown in Fig. 6, where the volume fraction of the recrystallized grains increases with the solution temperature increasing from 450 °C to 490 °C. The volume fraction of the recrystallized grains is less than 10% below 480 °C, but increased significantly to about 86% at 490 °C. The optical microstructures of the EST and HTPT samples undergo a partial recrystallization with the volume fraction of the recrystallized grains less than 10%, which is similar to that of the SST470 sample.

The sub-grain micrographs of the 7050 aluminum alloy solution treated at different conditions are shown in Fig. 7. For the SST440 sample, the sub-grains can be distinguished even though a large number of dislocations surround them. And the size of the sub-grains is about 1–3 μm. The contrasts within sub-grain regions appear uniform; a typical sub-microstructural feature of recovery. The sizes of the sub-grains increase remarkably with the solution temperature increasing from 440 °C to 490 °C (Fig. 7a–d). For the EST and the HTPT samples, the size of the sub-grains is similar to that of the SST460 sample.

Fig. 8 shows the typical fracture surfaces of the aged compact-tension specimens solution treated at different conditions. For the SST450 sample, decohesion and fracture of the residual second phase appears at the fracture surface. During deformation, some voids generally form on the interfaces between the residual phase and the matrix. As the plastic deformation proceeds, the growth and coalesce of the voids provide the fracture sources [5,9]. For the SST470 sample, there are many dimples on the fracture surface, which indicates that the failure is the ductile fracture. Therefore, the sample has a better fracture toughness. For the SST490 sample, there are copious recrystallized grains with the high angle grain boundaries which is the prefer propagation paths for the cracks [15–17]. Therefore, the fracture surface of the SST490 sample indicates a prevailing of intergranular fracture. The fracture toughness of the EST sample is higher than that of the SST470 sample. This explains why the dimples are bigger and deeper in Fig. 7d than those of Fig. 7b. It is in good accordance with the result of Fig. 4. The fracture surfaces of the HTPT sample also indicate the fracture of the residual second phase.

As above discussion, an improved tensile strength and fracture toughness can be achieved by proper solution treatment. Solution at low temperature is beneficial to the recovery and lead to the fine grains, and solution at high temperature is beneficial to the dissolving of the residual phase. A proper solution temper is essential for the heat treatment of the 7050 aluminum alloy.

It is obvious that the strengthening mechanisms for the 7050 aluminum alloy are mainly precipitation strengthening and fine grain strengthening when solution treated at different conditions and then aging treated at the same condition. The precipitation strengthening is ascribed to the dissolving of the second phase particles during the solution treatment, which offer great amounts of solution atoms and is beneficial for the precipitation in the subsequent aging treatment [9,18,19]. With increasing the solution temperature, more and more residual phase are dissolved into the matrix, providing more and more solution atoms, which results in a higher strength of the 7050 aluminum alloy. But the volume fraction of the recrystallized grains and the size of the sub-grains increases significantly with increasing the solution temperature, leading to a larger average grain size and a lower fine grain strengthening according to Hall–Petch relationship. As a result, with increasing the solution temperature, the tensile strength is a balance of the precipitation strengthening and the fine grain strengthening for the 7050 aluminum alloy, which can be described by Fig. 9a. It can be seen from Fig. 9a that the precipitation strengthening increases with increasing the solution temperature while the fine grain strengthening decreases. The comprehensive strength of the single-stage solution treated 7050 aluminum alloy reached the peak at the solution treatment of 470 °C. For the EST sample, the lower temperature solution promote the recovery of the alloy which inhibits the recrystallization in the following heat treatment, and the higher temperature solution dissolve the residual phase as more as possible. The EST sample has the best combination of the precipitation strengthening and the fine grain strengthening, which lead to a higher strength than the maximum of the single-stage

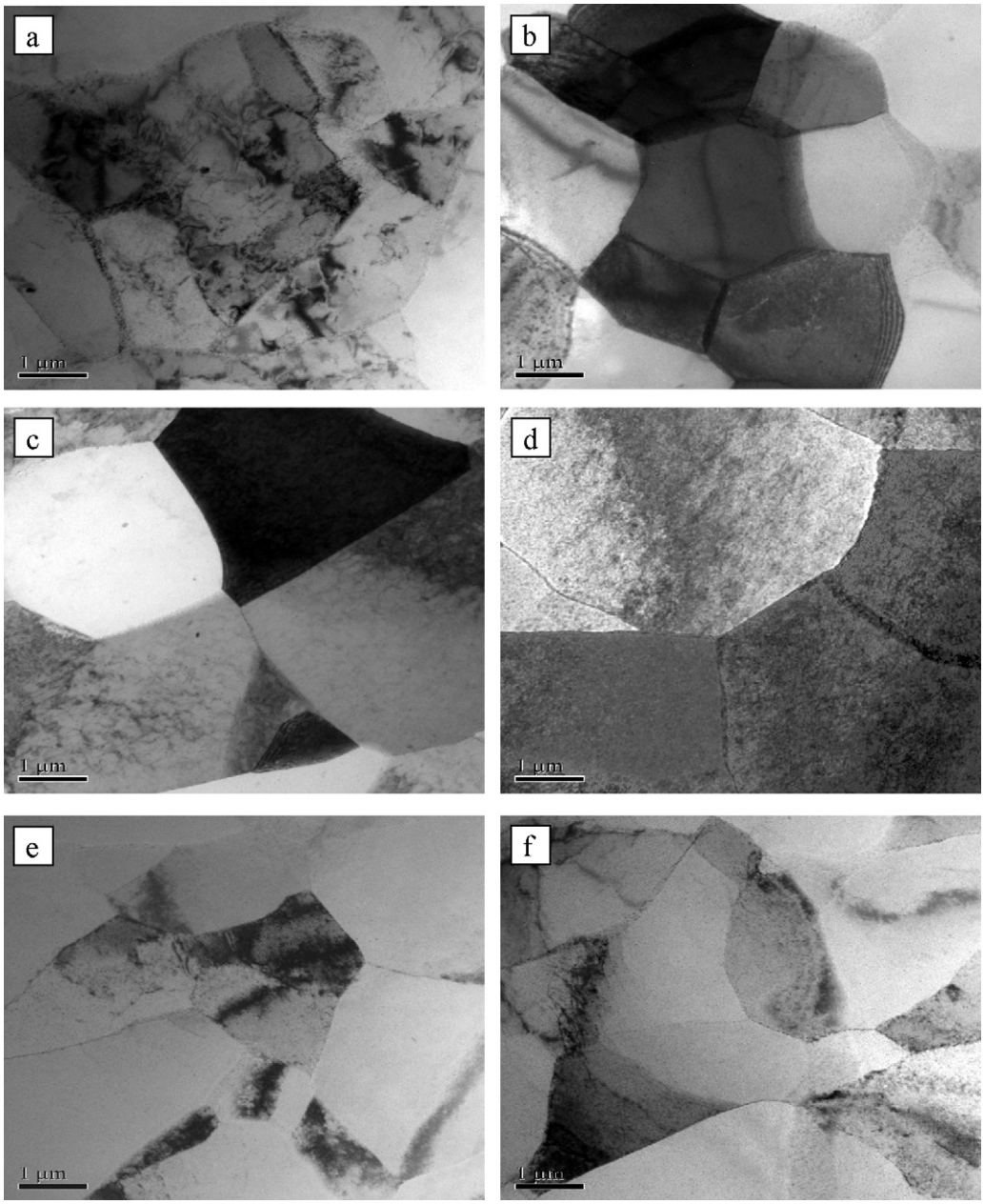

Fig. 7. TEM micrographs of the 7050 aluminum alloy solution treated at different conditions (a) SST440; (b) SST460; (c) SST470; (d) SST490; (e) EST and (f) HTPT.

solution treated sample. The grain structure of the HTPT sample is similar to that of the EST sample, however, a mass of fine AlZnMgCu phases precipitates from the matrix, which reduces the precipitation strengthening of the alloy. And the strength of the HTPT sample is only similar to that of the SST440 sample.

Similar to the strengthening mechanisms, the fracture mechanisms for the 7050 aluminum alloy solution treated at different conditions are controlled by the second phase particles and the grain structure. Second phase particles is usually the void/crack sources or the preferential crack paths and the samples show marked fall of fracture toughness as the volume fraction of the second phase particles increases [16,17]. With increasing the solution temperature, more and more second phase is dissolved, reducing the favorable nucleation sites for voids, which results in the increasing of the fracture toughness, illustrated as Fig. 9b. Meanwhile, the size of the sub-grains and the volume fraction of the recrystallized grains increase significantly with increasing the solution temperature which leads to a larger average grain size and the decreasing of the fracture toughness [20,21]. Especially, the high angle grain boundaries of the recrystallized grains are the prefer propagation path for the crack and the fracture toughness decrease with the increasing of the volume fraction of the recrystallized grains. The comprehensive fracture toughness of the single-stage solution treated 7050 aluminum alloy reached the peak at the solution treatment of 480 °C. The volume fraction of the second phase particles of the EST sample is similar to those of the SST490 sample, and the grain structure is similar to those of SST460 sample, which lead to a higher fracture toughness than the maximum of the single-stage solution treatment sample. The grain structure of the HTPT samples is similar to that of the EST samples, however, a mass of AlZnMgCu phases precipitates from the matrix, which reduce the fracture toughness.

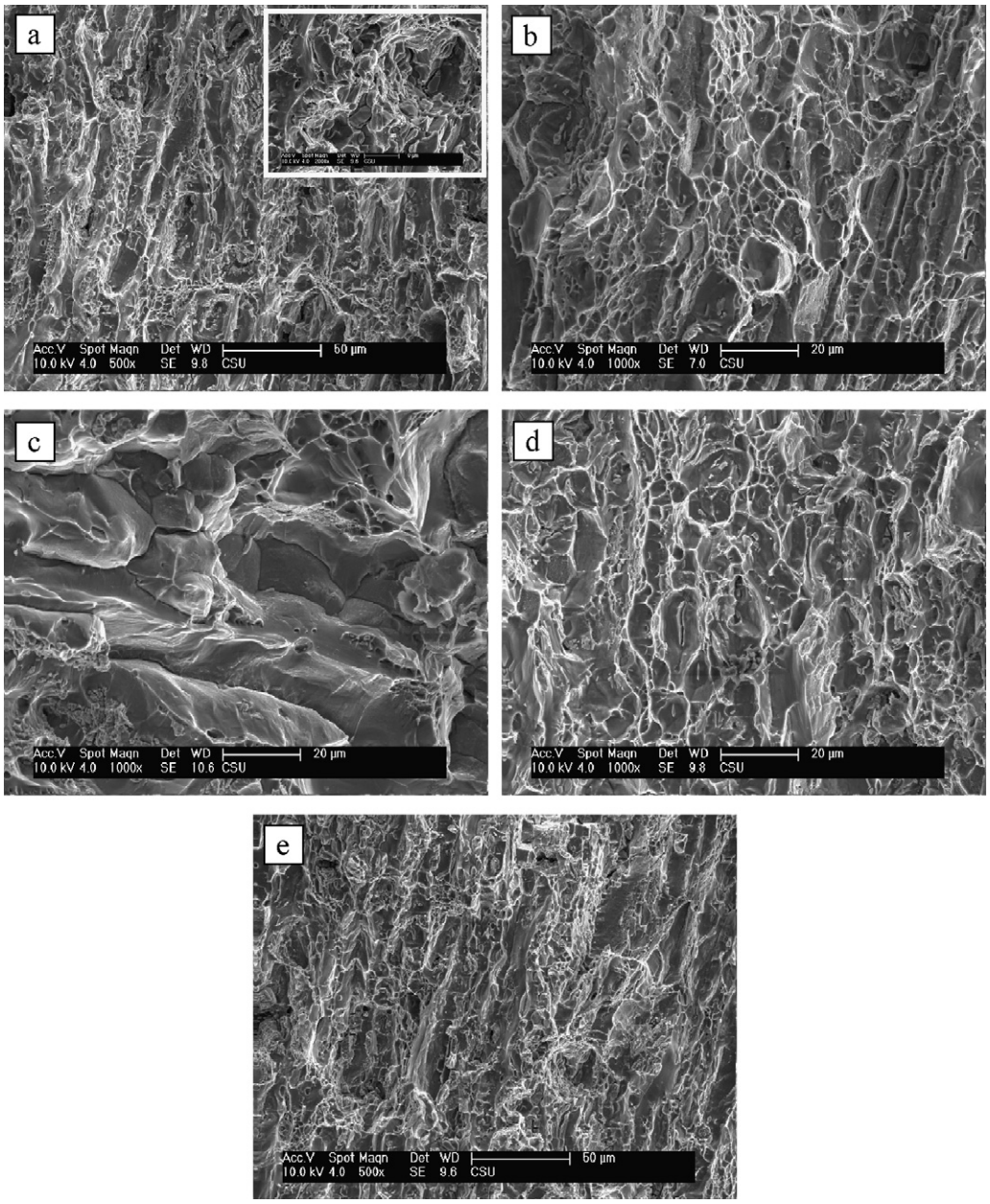

Fig. 8. Fracture surfaces of the aged 7050 aluminum alloy solution treated at different conditions (a) SST450; (b) SST470; (c) SST490; (d) EST and (e) HTPT.

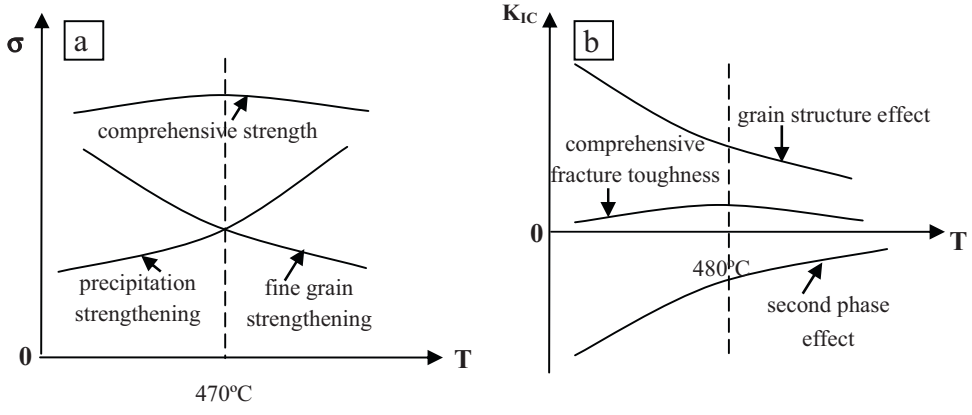

Fig. 9. Schematic diagram of (a) the strengthening mechanism and (b) the fracture mechanism of the single-stage solution treated 7050 aluminum alloy.

4. Conclusions

(1) The residual phase can be re-dissolved into the matrix with increasing the solution temperature, meanwhile, the volume fraction of the recrystallized grains and the size of the sub-grains increases dramatically. Therefore, the strength and fracture toughness of the single-stage solution treated samples increase first and then decrease with increasing the solution temperature.
(2) The application of the enhanced solution treatment is found to be effective in decreasing the volume fraction of the second phase particles and the grain size, and hence in comprehensively improving the strength and fracture toughness of the 7050 aluminum alloy.
(3) A mass of AlZnMgCu phases precipitates from the matrix of the high temperature pre-precipitation treated sample, which lead to a poor strength and fracture toughness.

Acknowledgments

The authors would like to appreciate the financial supports from State Key Fundamental Research Program of China (No. 2005CB623706), National Natural Science Foundation of China (Nos. 50230310 and 50905188).

References

[1] A. Heinz, A. Haszler, C. Keidel, S. Moldenhauer, R. Benedictus, W.S. Miller, Mater. Sci. Eng. A 280 (2000) 102–107.
[2] E.A. Starke Jr., J.T. Staley, Prog. Aerospace Sci. 32 (1996) 131–172.
[3] Y.L. Wu, F.H. Froes, A. Alvarez, C.G. Li, J. Liu, Mater. Des. 18 (1997) 211–215.
[4] Z.H. Li, B.Q. Xiong, Y.A. Zhang, B.H. Zhu, F. Wang, H.W. Liu, J. Mater. Process. Technol. 209 (2008) 2021–2027.
[5] Z. Cvijović, M. Rakin, M. Vratnica, I. Cvijović, Eng. Fract. Mech. 75 (2008) 2115–2129.
[6] D.K. Xu, N. Birbilis, D. Lashansky, P.A. Rometsch, B.C. Muddle, Corros. Sci. 53 (2011) 217–225.
[7] Y.L. Deng, L. Wan, Y. Zhang, X.M. Zhang, J. Alloys Compd. 498 (2010) 88–94.
[8] T. Hiroyuki, N. Takanori, U. Kentaro, S. Yoshio, K. Masakazu, Acta Mater. 58 (2010) 2014–2025.
[9] G. Liu, J. Sun, C.W. Nan, K.H. Chen, Acta Mater. 53 (2005) 3459–3468.
[10] K.H. Chen, H.W. Liu, Z. Zhang, J. Mater. Process. Technol. 142 (2003) 190–196.
[11] L.P. Huang, K.H. Chen, S. Li, M. Song, Scripta Mater. 56 (2007) 305–308.
[12] J.D. Robson, P.B. Prangnell, J. Mater. Sci. Technol. 18 (2002) 607–619.
[13] E.E. Underwood, Quantitative Stereology, Addison-Wesley, Reading, MA, 1970.
[14] D.L. Zhang, L.H. Zheng, D.H. St John, J. Light Met. 2 (2002) 27–36.
[15] A.M. Gokhale, N.U. Deshpande, D.K. Denzer, J. Liu, Metall. Mater. Trans. A 29 (1998) 1203–1210.
[16] R.C. Dorward, D.J. Beemtsen, Metall. Mater. Trans. A 26 (1995) 2481–2484.
[17] B. Morere, J.C. Ehrström, P.J. Gregson, I. Sinclair, Mater. Sci. Eng. A 31 (2000) 2503–2515.
[18] Z. Zhu, M.J. Starink, Mater. Sci. Eng. A 488 (2008) 125–133.
[19] M. Dixit, R. Mishra, K.K. Sankaran, Mater. Sci. Eng. A 478 (2008) 163–172.
[20] H. Erhard, G. Michael, Acta Metall. 25 (1977) 877–881.
[21] E. Hornbogen, E.A. Starker Jr., Acta Metall. Mater. 41 (1993) 1–16.